

Supporting Information

Anatomy of Screw Dislocations in Nanoporous SAPO-18 as revealed by Atomic Force Microscopy

Rachel L. Smith,^a Anna Lind,^b Duncan Akporiaye,^b Martin P. Attfield,^a
and Michael W. Anderson^{a,*}

^a Centre for Nanoporous Materials, School of Chemistry, The University of Manchester, Oxford Road, Manchester M13 9PL, UK

^b SINTEF Materials and Chemistry, P.O. Box 124, Blindern, 0314 Oslo, Norway

Contents

Figure S1. X-ray diffraction data of as-synthesised SAPO-18 (top) and reference AEI (bottom).	S2
Figure S2. Scanning electron microscopy image of SAPO-18 showing the square platelet morphology.	S2
Figure S3. Additional vertical deflection images of SAPO-18 crystals.	S3
Figure S4. a) Original image from Figure 2a with no rotation or marked terraces; b) cross section corresponding to the grey dotted line; c) cross section corresponding to the white dotted line across the interlaced feature.	S3
Figure S5. a) Q3 sites for the first configuration of A and B layers; b) the same configuration if the D6R is not present, which would not be the case as it increases the number of Q3 sites from 4 to 6; c) Q3 sites for the second configuration.	S4
Figure S6. a) Q3 sites on the corner in the first configuration of A and B layers; b) Q3 sites on the corner in the second configuration of A and B layers. Only visible Q3 sites are labelled as some Q3 sites are hidden from view due to the shape of the AEI-cage.	S4
Figure S7. Schematic showing the split step formed from equilibrium dissolution of the terrace to the most stable configuration. The dotted line shows the step before dissolution. Although the split step is higher energy than the original steps, the overall distance is shorter. This makes the dissolution favourable close to equilibrium.	S5
Figure S8. a) AFM image from dissolution of SAPO-18 shown in Figure 4a; b) cross section corresponding to the white dashed line on a).	S5
Experimental Details	S6

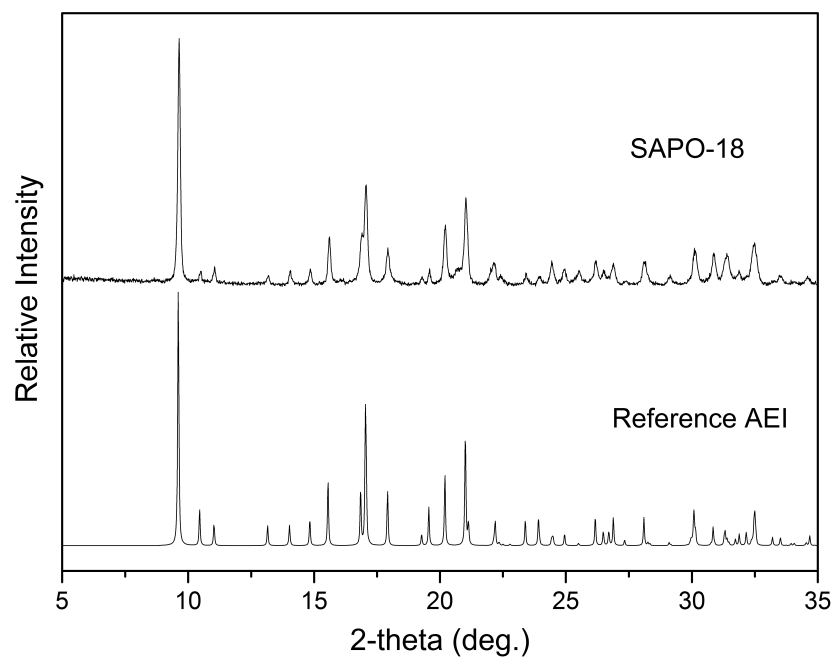


Figure S1. X-ray diffraction data of as-synthesised SAPO-18 (top) and reference AEI (bottom).

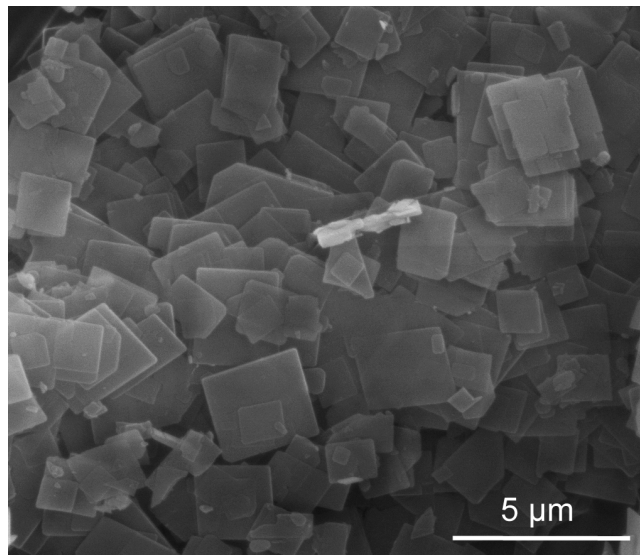


Figure S2. Scanning electron microscopy image of SAPO-18 showing the square platelet morphology.

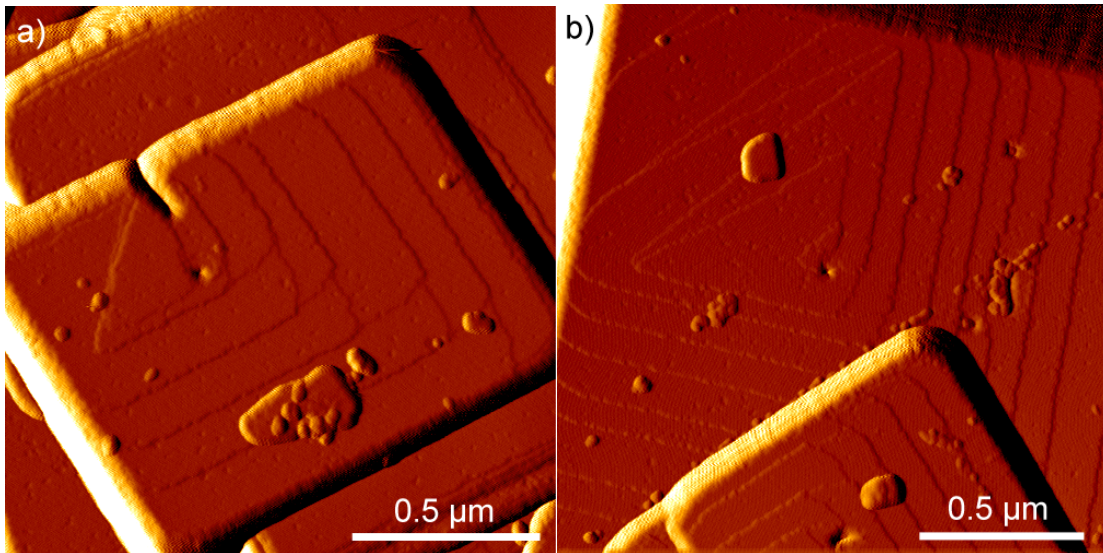


Figure S3. Additional vertical deflection images of SAPO-18 crystals.

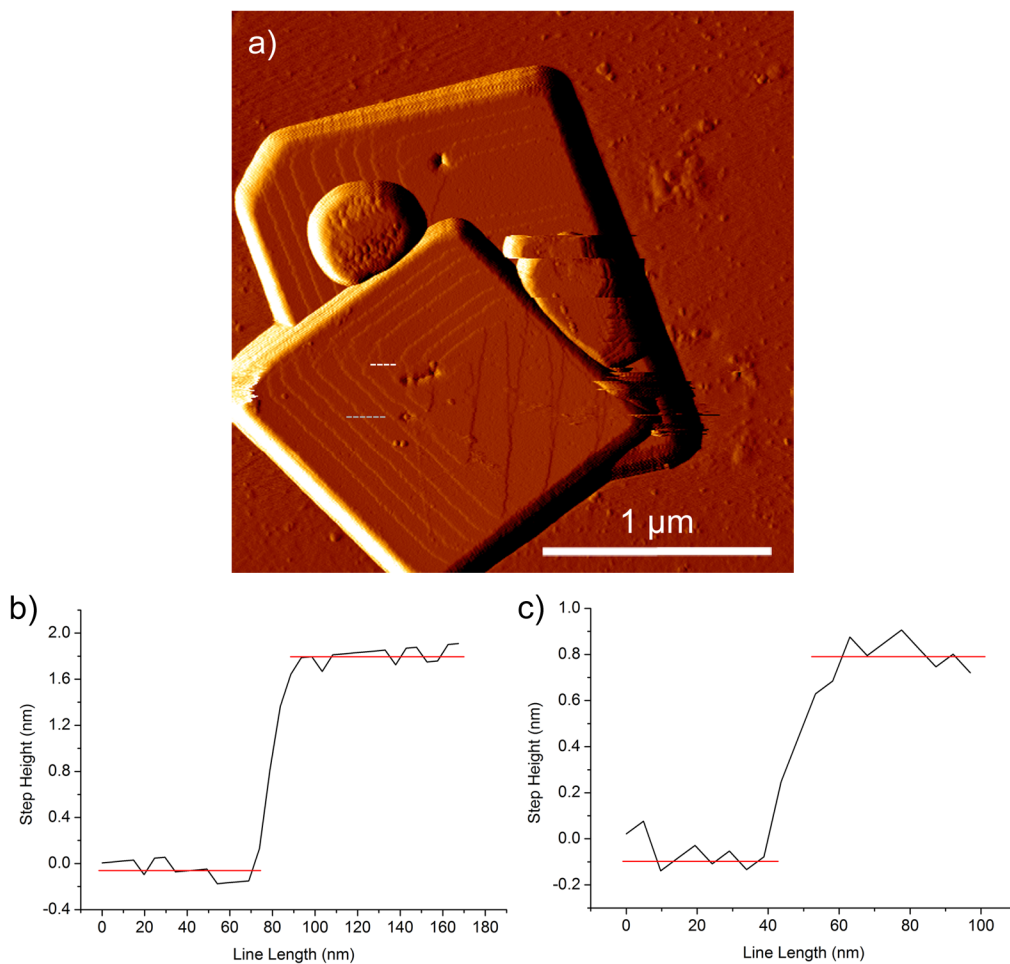


Figure S4. a) Original image from Figure 2a with no rotation or marked terraces; b) cross section corresponding to the grey dotted line; c) cross section corresponding to the white dotted line across the interlaced feature.

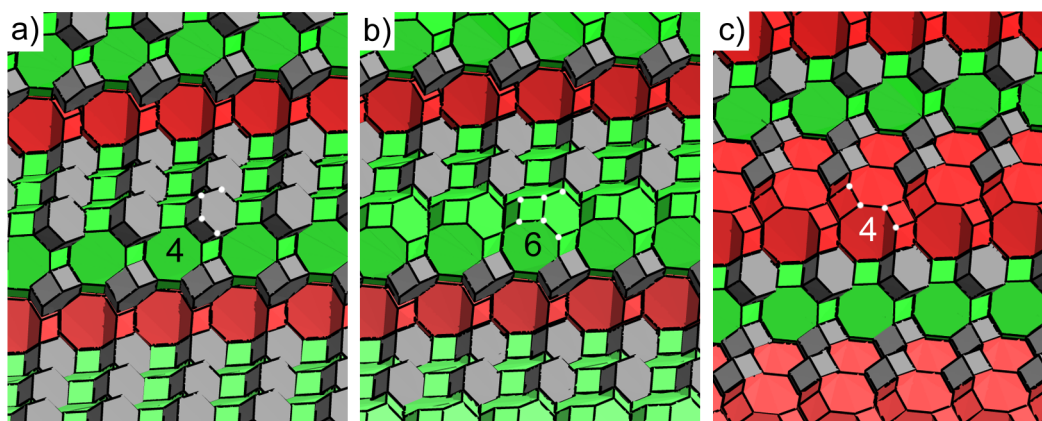


Figure S5. a) Q3 sites for the first configuration of A and B layers; b) the same configuration if the D6R is not present, which would not be the case as it increases the number of Q3 sites from 4 to 6; c) Q3 sites for the second configuration. Both configurations result in four Q3 sites.

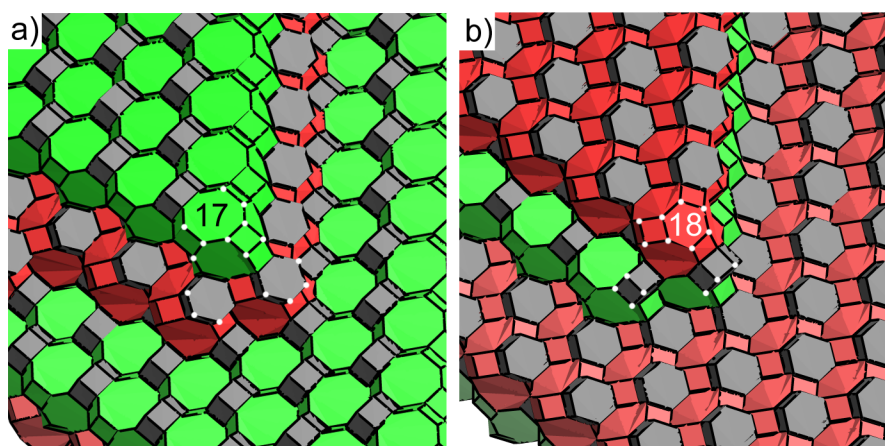


Figure S6. a) Q3 sites on the corner in the first configuration of A and B layers; b) Q3 sites on the corner in the second configuration of A and B layers. Only visible Q3 sites are labelled as some Q3 sites are hidden from view due to the shape of the AEI-cage.

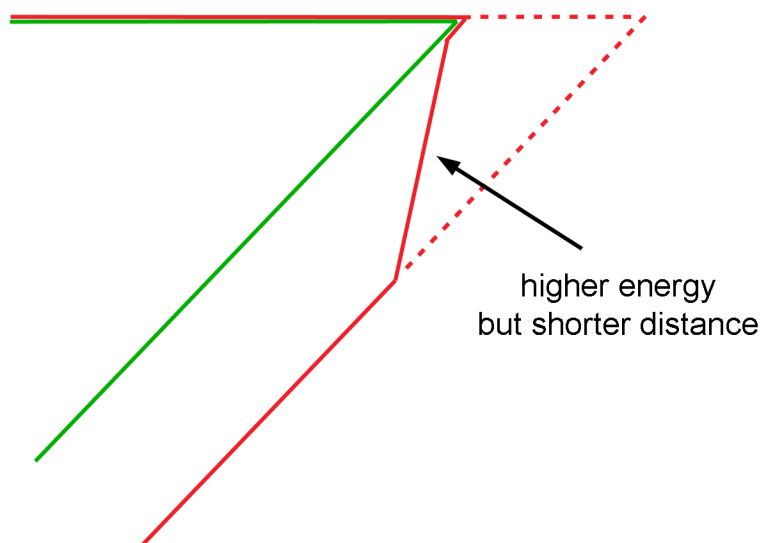


Figure S7. Schematic showing the split step formed from equilibrium dissolution of the terrace to the most stable configuration. The dotted line shows the step before dissolution. Although the split step is higher energy than the original steps, the overall distance is shorter. This makes the dissolution favourable close to equilibrium.

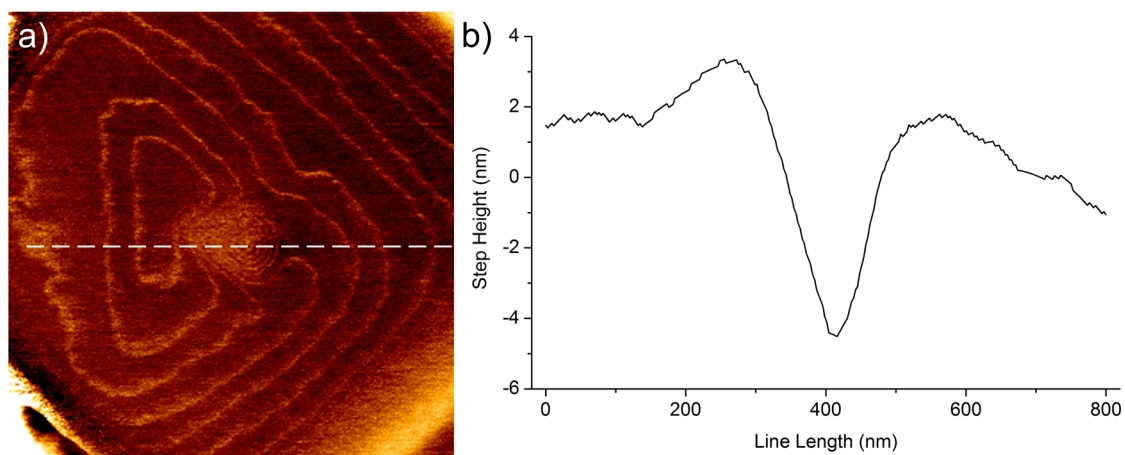


Figure S8. a) AFM image from dissolution of SAPO-18 shown in Figure 4a; b) cross section corresponding to the white dashed line on a).

Experimental Details

SAPO-18 was synthesised according to the synthesis route reported by Mertens *et al.*¹ The molar ratio of the final gel was 0.01 SiO₂ : 1 Al₂O₃ : 1 P₂O₅ : 1 TEAOH : 35 H₂O. A mixture of phosphoric acid, (85%, Merck), tetraethyl ammonium hydroxide (TEAOH, 35%, Sigma Aldrich) and deionised water was heated to 30°C and Ludox-AS-40 (40% SiO₂, DuPont) and Pural SB (76% Al₂O₃, SASOL) were added under continuous stirring before aging at 30°C for 2 h with stirring. The aged gel was transferred to Teflon-lined autoclaves and heated to 165 °C (heating rate 5 °C/h) and maintained for 72 h with rotation. The reaction was quenched in water and the product separated by centrifugation. The product was washed with deionised water and dried at 95 °C overnight.

AFM was performed in contact mode in air on a JPK Nanowizard II Bio-AFM mounted on an inverted Axiovert 200 MAT optical microscope. Silicon nitride tips (Bruker probes NP-10, spring constant 0.58 Nm⁻¹) were used with a scan rate of 1-2 Hz. *In-situ* dissolution was carried out in the JPK BioCell in static phosphoric acid solution (pH 5) using a scan rate of 4.5 Hz. Images were processed using the JPK Data Processing software. Graphics have been produced by in-house software using Mathematica 8.0.1.

¹ M. M. Mertens. World Patent 2009/117186, February 6, 2009